Band structures in ^{106}Pd

C. Y. He (贺创业),[1] B. B. Yu (于蓓蓓),[1] L. H. Zhu (竺礼华),[2,*] X. G. Wu (吴晓光),[1,†] Y. Zheng (郑云),[1] B. Zhang (张彪),[1] S. H. Yao (姚顺和),[1] L. L. Wang (王烈林),[1] G. S. Li (李广生),[1] X. Hao (郝昕),[1] Y. Shi (石跃),[3] C. Xu (徐川),[3] F. R. Xu (许甫荣),[3] J. G. Wang (王建国),[4] L. Gu (顾龙),[4] and M. Zhang (张明)[4]

[1]*China Institute of Atomic Energy, Beijing 102413, China*

[2]*School of Physics and Nuclear Energy Engineering, Beihang University, Beijing 100191, China*

[3]*Department of Technical Physics and MOE Key Laboratory, Peking University, Beijing 100871, China*

[4]*Department of Physics, Tsinghua University, Beijing 100084, China*

(Received 19 June 2012; revised manuscript received 4 September 2012; published 1 October 2012)

The high spin states of ^{106}Pd have been investigated with in-beam γ-ray spectroscopic methods using the ^{100}Mo(^{11}B, $1p4n$)^{106}Pd reaction at a beam energy of 60 MeV. All earlier known bands were extended considerably and additional bands were identified. The configurations of these bands are discussed on the basis of the experimental aligned angular momenta and total Routhian surface calculations. Both two-quasineutron and two-quasiproton structures have been found in ^{106}Pd. The nonyrast low-lying positive-parity band was interpreted as a γ-vibrational band.

DOI: 10.1103/PhysRevC.86.047302 PACS number(s): 21.10.Hw, 25.70.Jj, 23.20.Lv, 21.10.Re

The $A \sim 110$ mass region is a fertile land for experimental investigation of nuclear structure. For example, it is of particular interest for studying γ-vibrational bands, pesudospin doublet bands, and chiral bands in this region. A series of experiments [1–7] have been performed at the China Institute of Atomic Energy (CIAE) to search for such bands in neutron-deficient nuclei close to $Z \sim 45$. But no chiral bands have been found in the even-even nuclei. Recently, calculations of the potential energy surface (PES) obtained by using a Hartree-Fock + BCS + Lipkin-Nogami procedure [8] predict a prolate shape for ^{106}Pd with increasing softness in γ and β directions. In this background, vibrational bands could come into being. It is also very interesting to investigate chiral bands since ^{106}Pd lies near the island center of chirality.

Shape and phase evolution are also central themes in nuclear structure research. This evolution is intimately related to the mechanisms by which atomic nuclei generate angular momentum. ^{106}Pd is situated between the well-deformed nuclei and the $Z = 50$ shell closure. Therefore, it is very meaningful to study how deformation evolves in ^{106}Pd from low to high spin states.

Some of the high spin levels in ^{106}Pd have been established from the ^{96}Zr(^{13}C, $3n$) reaction [9]. In that experiment, many γ transitions in ^{106}Pd were subsequently identified and placed into band structures by measuring prompt γ rays using two Ge(Li) detectors positioned 3 cm from the target. At the same time, liner polarization measurements in conjunction with angular distribution data performed by Stromswold *et al.* [10] were used to assign negative parity to the side band in ^{106}Pd. In this work, we present results of an investigation of ^{106}Pd with the ^{100}Mo (^{11}B, $1p4n$) reaction.

High spin states in ^{106}Pd were populated through the ^{100}Mo (^{11}B, $1p4n$) reaction at a beam energy of 60 MeV. The target consisted of a 1.56 mg/cm^2 foil of ^{100}Mo (isotopically enriched to 97.4%) onto a 8.03 mg/cm^2 natural lead backing. The ^{11}B beam was delivered by the CIAE HI-13 tandem accelerator. The γ rays were detected by ten Compton-suppressed HPGe detectors, two low-energy photon (LEP) detectors, and one clover-type detector. The Ge detectors in the array were placed at 90°, ±37°, ±30°, and ±60° relative to the beam direction. Each detector had an energy resolution of about 2 keV for 1332.5-keV γ rays. Energy and efficiency calibrations of the detectors were performed using the standard sources ^{60}Co and ^{152}Eu. Coincidence data have been recorded in an event-by-event mode when at least two signals from HPGe detectors were generated in 200 ns. A total of 230×10^6 γ-γ coincidence events were recorded. The data were sorted into a fully symmetrized E_γ-E_γ coincidence matrix, as well as into an asymmetric directional correlation ratio of oriented states (DCO) matrix. The DCO matrix was created by sorting the detectors at ±37° on one axis and the detectors at ∼90° on the other. These matrices were analyzed with the RADWARE program [11]. In our array geometry, if one gates on a stretched quadrupole transition, the expected DCO ratios are close to 1.0 for stretched quadrupole transitions and around 0.6 for pure dipole transitions. Spin and parity assignments of excited states were based, where possible, on this empirical observation for the de-exciting γ transitions.

The level scheme of the ^{106}Pd nucleus deduced from the present work is shown in Fig. 1. This level scheme is based on the coincidence relationships, intensity balances for each level, and energy sums from different paths using the symmetrized E_γ-E_γ coincidence matrix, and it is essentially in agreement with earlier work [9]. Prior to this work, firm knowledge of the ^{106}Pd yrast level scheme was limited to states with spin up to $16\hbar$ and only two band structures were established. In the present experiment, the level scheme of ^{106}Pd are constructed into six bands. Besides the known γ transitions, 26 new γ rays and 15 new levels are found in our experiment. Figure 2 shows sample spectra, which are produced by gating on the 732-, 1618-, and 960-keV lines, for the logic of the construction of the negative-parity side bands. The new transitions at 1001, 960, and 1018 keV are observed in the corresponding spectrum gated at 732 and 1618 keV, whereas, for example, in the

*zhulh@buaa.edu.cn
†wxg@ciae.ac.cn

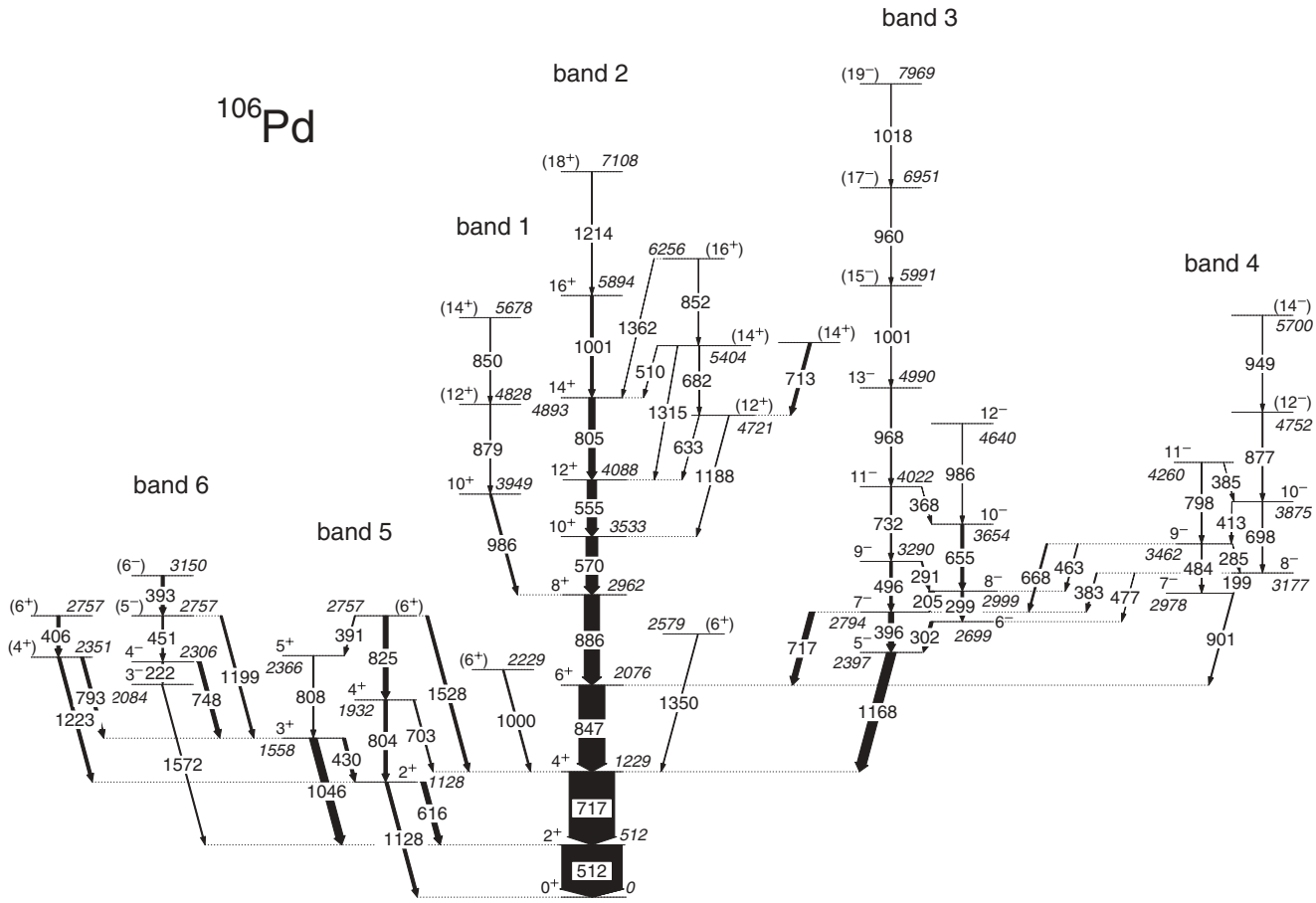

FIG. 1. Deduced new level scheme of ^{106}Pd from the present experiment. The γ energies are in keV. The widths of the arrows are proportional to the intensities of the transitions.

960-keV-gated spectrum, together with the new transitions at 1001 and 1018 keV, the known γ rays in this sequence, such as 732, 1618, 496, and 968 keV, are also clearly identified. This proves that the transitions at 1001, 960, and 1018 keV are members of band 3. In addition, the new transitions at 877 and 949 keV are also distinguished in the 1618-keV-gated spectrum. This thus proves the existence of 877- and 949-keV lines in the negative-parity side bands.

The yrast band 2 is extended up to spin $18^{+}\hbar$. An alignment is observed with $10\hbar$ increasing in angular momentum (shown in Fig. 3) compared with the ground state, in which the Harris parameters used for reference, taken from Ref. [12], are $J_0 = 6\hbar^2\,\mathrm{MeV}^{-1}$ and $J_1 = 20\hbar^4\,\mathrm{MeV}^{-3}$. This is a ubiquitous phenomenon in the yrast bands of even-even nuclei of the $A \sim 110$ mass region. The large alignment in band 2, therefore, may result from the alignment of one pair of $h_{11/2}$ neutrons. The empirical a ratio of E_γ over spin (E-GOS) curve [13], which is an empirical approach to distinguish vibrational from rotational regimes in atomic nuclei, is also provided in Fig. 4 for band 2. The ratios of E_γ/I for band 2 decrease with spin and incline to zero below $10\hbar$, then lower spin states appear in band 2 to be built on a vibrational mode. However, the E-GOS ratios for the states beyond spin $10\hbar$ tend to be a constant value. The constant values of E-GOS ratios imply a collective character for band 2 at higher spin states. On the other hand, the occupation of the $\nu h_{11/2}$ subshell induces a stabilization of the shape of ^{106}Pd, and one can see in Fig. 3 that the experimental alignments have nearly constant alignment after band crossing. One should note that the band crossing happens around the same spin point as the inflection of E-GOS curve. The transition from vibrational mode to collective mode could therefore be a result of the band crossing.

The low-lying cascade, which is labeled with band 5 in Fig. 1, established on the second 2^+ state is assigned as the γ-vibrational band since this kind of collective motion is a common feature in even-even Pd isotopic nuclei [14,15]. Recently, such a structure has been identified also in ^{104}Pd [16], and it was interpreted as a quasi-γ band associated with γ-soft deformation. In order to further understand the shape of ^{106}Pd, the staggering signature defined as [17]

$$S(I, I-1, I-2) = \frac{E(I) + E(I-2) - 2E(I-1)}{E(2_1^+)} \qquad (1)$$

has been calculated. It is a good indicator for distinguishing between γ-soft and γ-rigid potentials. When the staggering gives positive values, the potential is triaxial rigid; when it is negative it is γ-soft. The experimental odd-even spin energy staggering deduced for band 5 is displayed in Fig. 5 together with the values extracted for ^{104}Ru [18]. It is clear that the even spin has negative values, while the odd spin has positive values, which is the same as occurs in ^{104}Pd [16]. Thereby,

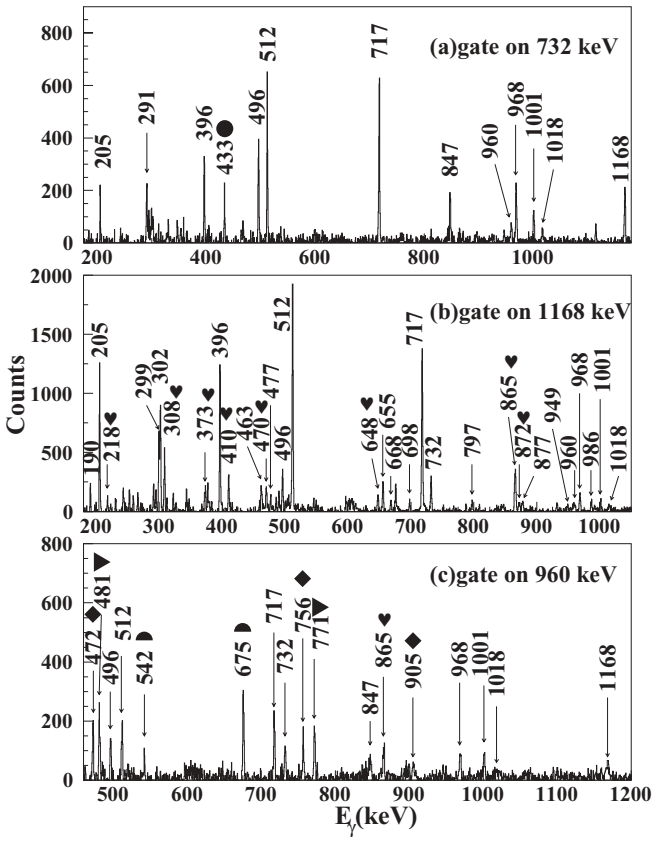

FIG. 2. Sample spectra gated by 732, 1168, and 960 keV. Peaks without any symbols belong to ^{106}Pd. The energies marked by the closed circle, semicircles, heart symbols, triangles, and diamonds are contaminants from ^{105}Ag, ^{106}Ag, ^{107}Ag, ^{105}Pd, and ^{107}Pd, respectively.

one can rule out the γ-rigid potential scenario for ^{106}Pd. On the other hand, cranked Woods-Saxon-Strutinsky calculations have also been performed by means of total Routhian surface (TRS) methods in a three-dimensional deformation space (β_2, β_4, γ) [19,20]. At a given frequency, the deformation of a state is determined by minimizing the resulting total Routhian surfaces. Figure 6(a) displays a prolate shape for the vacuum configuration of ^{106}Pd nuclei. The minimum is located at

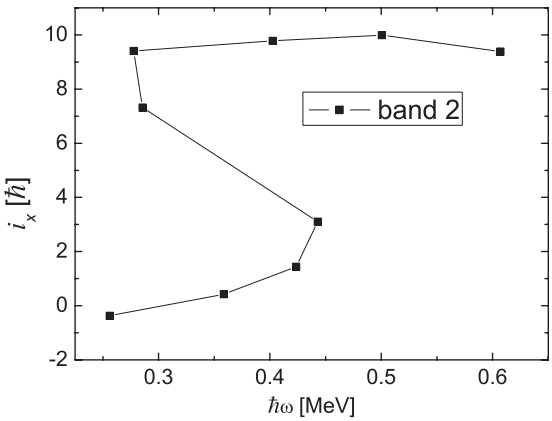

FIG. 3. Experimental alignment as a function of rotational frequency ω for bands 1 and 2 in ^{106}Pd.

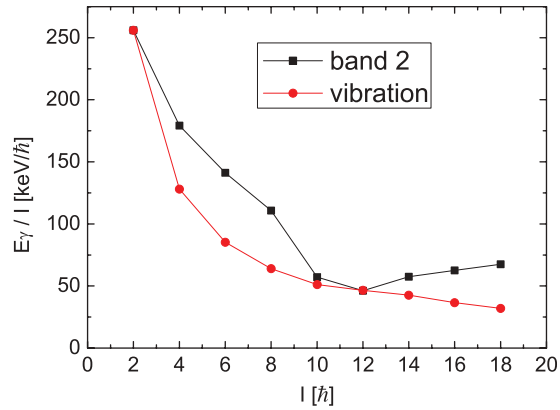

FIG. 4. (Color online) Empirical E-GOS plot for bands 1 and 2 in ^{106}Pd.

$\gamma \approx 0$, but with large softness in the γ direction. This statement is in agreement with the results of the staggering signature calculation. In addition, the $E2$ transitions in band 5 remains nearly constant in energy. All this combined evidence above give a confident assignment to band 5 as a γ-vibrational band. It should be mentioned that the second 2^+ state was also interpreted as a two-phonon triplet state in Ref. [21]. This interesting phenomenon provides a challenge to theory and deserves further investigation by the nuclear physics community.

Bands 3 and 4 lie much higher in excitation energy than the ground band. They are very possibly built on two-quasiparticle configurations. ^{106}Pd nuclei have 46 protons and 60 neutrons. Based on filling of the Nilsson orbitals, the two quasiparticles are likely to arise from neutron $h_{11/2} \otimes g_{7/2}$, neutron $h_{11/2} \otimes d_{5/2}$, and proton $g_{9/2} \otimes p_{1/2}$ particle-hole states. If band 3 in the ^{106}Pd 5^- state comes from the quasiproton configuration, the excitations should be largely insensitive to changes in neutron number (N), while the energy of the 5^- state in its isotopes drops in energy with increasing N [14–16]. In this picture, band 3 would most likely be quasineutron excitations. Band 4 would also be of quasineutron origin since it has many linking transitions with band 3.

The levels with the same spin and parity in bands 3 and 4 lie very close in energy. Furthermore, the experimental alignments

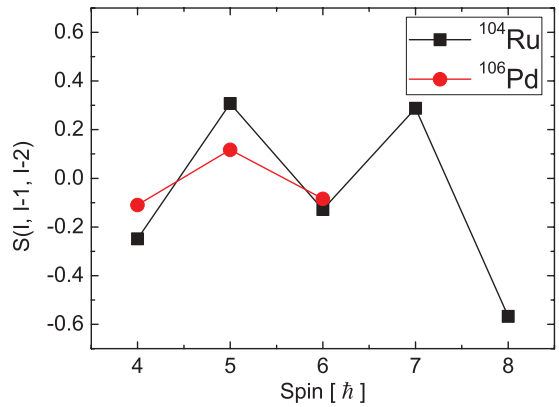

FIG. 5. (Color online) Experimentally observed odd-even spin energy staggering in band 5 together with the values of the quasi-γ band in ^{104}Ru.

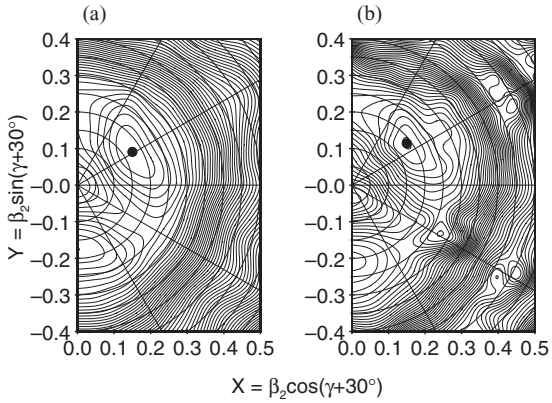

FIG. 6. Polar coordinate plots of TRS for ^{106}Pd. Contour lines are in 200-keV increments. (a) Vacuum: $\hbar\omega = 0.0$ MeV, with a minimum at $\beta_2 = 0.175$, $\beta_4 = -0.003$, $\gamma = 1.314°$. (b) $\nu h_{11/2} \otimes g_{7/2}/d_{5/2}$: $\hbar\omega = 0.25$ MeV, with a minimum at $\beta_2 = 0.189$, $\beta_4 = -0.003$, $\gamma = 7.228°$.

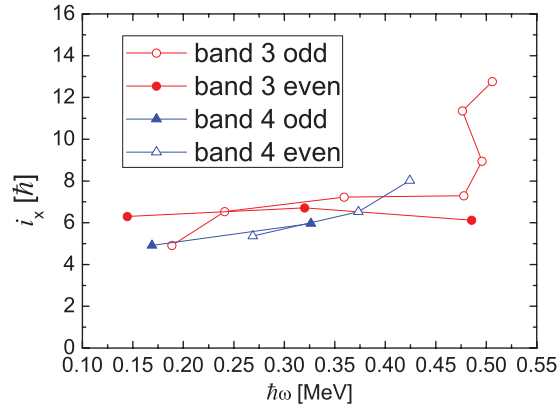

FIG. 7. (Color online) Experimental alignments of bands 3 and 4 in ^{106}Pd.

for those two bands presented in Fig. 7 are also very similar. It is possible that they could be a pair of chiral bands or pseudospin doublet bands. However, their γ deformation from a TRS calculation [in Fig. 6(b)] is too small to lead to chiral symmetry being broken. In addition, bands 3 and 4 exhibit considerable signature splitting, whereas in chiral bands the signature splitting curve goes relative smoothly with spin. Then, the assignment of chiral bands can be ruled out.

For small deformations, the neutron Fermi surface lies near the $g_{7/2}$ and $d_{5/2}$ multiplet orbitals. They are, however, usually strongly mixed, resulting from deformation and/or rotation, seen for example by comparison with its isotone ^{108}Cd [22] and adjacent isotopic nuclei ^{104,108}Pd [16,23]. From the Nilsson diagram, the orbitals with Nilsson quantum numbers 3/2[411] and 5/2[413] can be considered as a pair of pseudospin partners with pseudospin quantum numbers $(\tilde{\Omega}[\tilde{N}\tilde{n}_z\tilde{\Lambda}])5/2[\tilde{3}\tilde{1}\tilde{2}]$ and $3/2[\tilde{3}\tilde{1}\tilde{2}]$ [24]. Bands 3 and 4, therefore, could be described as pseudospin doublet bands with a $\nu h_{11/2} \otimes g_{7/2}/d_{5/2}$ configuration. This is the reason for the small difference between these two bands. The odd spin branch of band 3 continues to higher spins and is crossed by a four-quasiparticle band at $\hbar\omega \approx 0.5$ MeV. The observed gaining of angular momentum in Fig. 7 is about $7\hbar$. But we did not observe the end of the backbending in the present experiment. It is suggested that this band crossing is mainly coming from the excitation of two $h_{11/2}$ neutrons. By comparison with the yrast band, this crossing is delayed because of blocking of one of the $h_{11/2}$ neutrons.

The bandhead energy of band 6 has a value similar to that of band 3. It has been pointed out by using Hartree-Fock-Bogoliubov calculations [18] that the lowest two-proton and two-neutron states are expected to have similar excitation energy. The lowest two-proton quasiparticle state is the coupling between $\pi\ p_{1/2}$ and $\pi g_{9/2}$. Indeed, similar structure has been found in the neighboring isotopic nuclei ^{104}Pd [16]. Thereby, the configuration is assigned as proton $g_{9/2} \otimes p_{1/2}$.

In conclusion, the high spin states of the ^{106}Pd nucleus have been measured and the level scheme has been updated considerably. Band 2 has good rotational character after an alignment built on a pair of $h_{11/2}$ neutrons. Bands 3 and 4 could make a pseudospin doublet bands. Band 5 has γ-vibrational character. The newly constructed band 6 possibly originates from two-quasiproton excitation.

The authors are grateful to the crew of the CIAE HI-13 tandem accelerator for steady operation of the accelerator and to Dr. Q. W. Fan for preparing the target. This work is supported by the Major State Basic Research Development Program (Grant No. 2007CB815000) and by the National Natural Science Foundation of China (Grants No. 11175259, No. 11075214, No. 10927507, and No. 10975191).

[1] C. Y. He *et al.*, High Energy Phys. Nucl. Phys. **30**, 166 (2006) [in Chinese].
[2] C. Y. He *et al.*, Phys. Rev. C **81**, 057301 (2010).
[3] C. Y. He *et al.*, Phys. Rev. C **83**, 024309 (2011).
[4] C. Y. He *et al.*, Plasma. Sci. Technol. **14**, 518 (2012).
[5] C. Y. He *et al.*, At. Energy Sci. Technol. **45**, 129 (2011) [in Chinese].
[6] H. B. Ding *et al.*, Chin. Phys. Lett. **27**, 072501 (2010).
[7] S. Y. Wang *et al.*, Phys. Rev. C **82**, 057303 (2010).
[8] T. Venkova *et al.*, Eur. Phys. J. A **6**, 405 (1999).
[9] J. A. Grau *et al.*, Phys. Rev. C **14**, 2297 (1976).
[10] D. C. Stromswold *et al.*, Phys. Rev. C **13**, 1510 (1976).
[11] D. C. Radford, Nucl. Instrum. Methods **361**, 297 (1995).
[12] K. R. Pohl *et al.*, Phys. Rev. C **53**, 2682 (1996).
[13] P. H. Regan *et al.*, Phys. Rev. Lett **90**, 152502 (2003).
[14] S. Lalkovski *et al.*, Eur. Phys. J. A **18**, 589 (2003).
[15] K. Butler-Moore *et al.*, J. Phys. G **25**, 2253 (1999).
[16] D. Sohler *et al.*, Phys. Rev. C **85**, 044303 (2012).
[17] N. V. Zamfir and R. F. Casten, Phys. Lett. B **260**, 265 (1991).
[18] I. Deloncle *et al.*, Eur. Phys. J. A **8**, 177 (2000).
[19] W. Satula, R. Wyss, and P. Magierski, Nucl. Phys. A **578**, 45 (1994).
[20] F. R. Xu, W. Satula, and R. Wyss, Nucl. Phys. A **669**, 119 (2000).
[21] G. Gürdal *et al.*, Phys. Rev. C **82**, 064301 (2010).
[22] I. Thorslund *et al.*, Nucl. Phys. A **564**, 285 (1993).
[23] J. A. Alcántara-Núñez *et al.*, Phys. Rev. C **71**, 054315 (2005).
[24] A. Bohr, I. Hamamoto, and B. R. Mottelson, Phys. Scr. **26**, 267 (1982).